Raman and Infrared Microspectroscopy

Pina Colarusso, Linda H Kidder, Ira W Levin, and E Neil Lewis, National Institutes of Health, Bethesda, MD, USA

This article is reproduced from the previous edition, volume 3, pp 1945–1954, with revisions made by the Editor, © 1999, Elsevier Ltd.

Symbols

n	refractive index
NA	numerical aperture
M	magnification
p	pixel size
r_A	radius of the Airy disc
R	distance between two incoherent point sources
R_L	lateral spatial resolution
λ	wavelength of light
ϕ_{max}	half-angle of the maximum cone of light collected by the lens

Introduction

Vibrational Raman and infrared microspectroscopy are analytical tools that characterize both the chemistry and the physical structure of materials. These methods combine two separate approaches, vibrational spectroscopy and light microscopy, for elucidating chemical systems at the micron and the submicron levels. Whereas vibrational spectroscopy probes the details of molecular composition, light microscopy reveals sample morphology based on the variations in optical properties. Vibrational microscopy builds on both of these techniques, and thus provides chemically selective visualizations of microscopic samples. Domains within complex samples, ranging from diamond inclusions in a mineral to malignant cells in a tissue biopsy, may be examined with Raman and infrared techniques. The efficacy and flexibility of vibrational microspectroscopy is highlighted by its wide adoption in diverse areas such as geology, medicine, forensic science, and industrial process control.

Since the theoretical background and practical implementation of vibrational spectroscopy are described elsewhere in this encyclopedia, the emphasis here will be on the extension of Raman and infrared spectroscopy to the microscopic realm. It should be noted that many of the methods described here are applicable to other microspectroscopic methods, especially those based on optical phenomena such as fluorescence.

The balance between spectroscopy and microscopy distinguishes one vibrational microscopic technique from another. At one extreme, spectroscopic and microscopic analyses are carried out separately. In a typical arrangement, the sample is examined through a microscope under white-light illumination, and then either Raman or infrared spectra are recorded at one or more selected points. Approaches that more fully integrate the acquisition of morphological and spectroscopic data have also been developed. Mapping techniques record spectra at successive points or lines within the sample; the spectra are combined to provide a view of the sample at specific vibrational frequencies. Imaging techniques, by contrast, record spectra simultaneously for contiguous points within a given sample area.

Mapping and imaging methods allow for sample visualizations over sequential wavelength intervals. The data sets are represented by a three-dimensional 'image cube' having two spatial and one spectral dimension (see Figure 1). Depending on the orientation, two-dimensional slices along

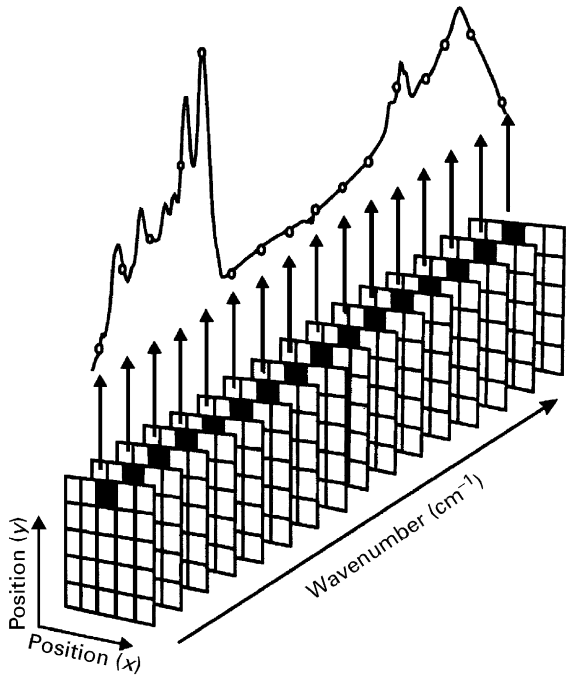

Figure 1 Mapping and imaging data can be depicted as an 'image cube' having two spatial and one spectral dimension.

a particular axis yield either a set of image planes stacked as a function of wavelength or a group of spatially resolved spectra. Vibrational spectroscopic mapping and imaging combine the morphological and chemical analyses of microscopic systems and reveal trends that are often difficult to extract from bulk or isolated single-point measurements.

Instrumentation

A standard Raman or infrared microspectrometer consists of an excitation source, a compound microscope, a spectrometer, and a detector. As in bulk techniques, the design of microspectroscopic experiments is guided by the sample composition as well as demands for frequency response, sensitivity, data acquisition rates and spectral resolution. Factors specific to vibrational microspectroscopy include the spatial resolution and the optical throughput between the microscope and the spectrometer.

Sources

Raman microspectroscopy is usually implemented from the ultraviolet to near-infrared wavelength regions, from approximately 0.3 to 1.5 μm. Excitation with sources such as Ar^+, HeNe and solid-state lasers is standard. Infrared microspectroscopy, by contrast, is usually carried out between 0.78 and 25 μm with broadband sources such as quartz lamps or ceramic globars. More recently, excitation with synchrotron radiation has also been demonstrated for infrared measurements.

The Compound Microscope

The compound microscope is central to vibrational microspectroscopy. The optical components and light paths for both refractive and reflective microscopes are shown in Figure 2. As illustrated, a compound microscope contains a light source, a condenser, an objective, various apertures and an ocular. The sample is first visualized under white light to aid in observation and alignment. The condenser illuminates the sample, and the transmitted light is collected by the objective. Light also can be reflected (or scattered) from the sample; in this configuration, which is known as epi-illumination, the objective also serves as the condenser. In either case, an inverted and usually enlarged image of the sample is formed at the back focal plane of the objective. This intermediate image is relayed either through collection optics to a video camera or through the ocular, which further magnifies the image for viewing. Microscopes tailored for operation at ultraviolet and infrared wavelengths usually contain a parfocal white-light path for sample observation.

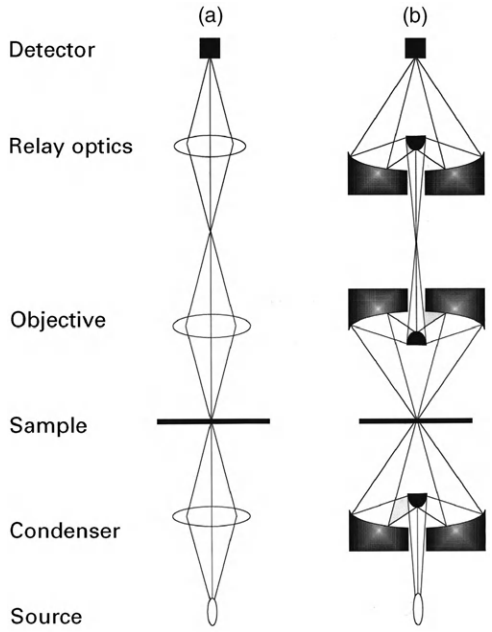

Figure 2 Schematics of (a) refractive and (b) reflective microscopes.

Following the preliminary microscopic examination, the spectroscopic source is introduced on to the sample. In Raman microspectroscopy, the probed region is defined by the size of the impinging laser beam. For infrared applications, the radiation is localized within a given area in part by placing an aperture between the source and the sample. An image of the irradiated area, corresponding to the Raman or infrared signal, is formed behind the objective, and is diverted to the spectrometer for analysis. The optical path of the vibrational signal is configured such that it focuses in the same plane as the white-light image; the parfocal light paths ensure that identical sample regions are examined in both procedures, while maximizing the optical throughput.

Microscope Lenses

Microscope lenses are complex assemblies that are designed to balance the requirements for magnification, focal length and light collection with various factors that degrade image fidelity (note that the optics in Figure 2 are simplified for clarity). Refractive and reflective optics exhibit aberrations that cause image blurring and deformation. These include effects such as spherical aberrations and astigmatism. Refractive optics also exhibit chromatic aberrations which cause light of different wavelengths to focus at separate points.

The highest-quality images are generally obtained with light microscopes that contain refractive glass elements. Visible Raman microspectroscopy, in particular, benefits from the mature optical technology that has been developed for visible wavelengths. Refractive optics are

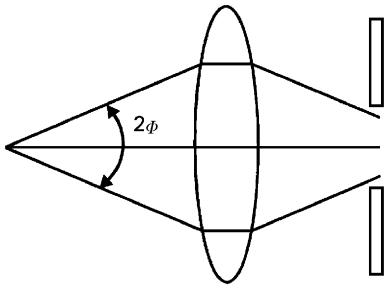

Figure 3 The numerical aperture is defined as $n \sin \phi$, where n is the refractive index of the surrounding medium and ϕ is the half-angle of the cone of light collected by the optic.

available for vibrational microspectroscopic applications at other wavelengths; examples include quartz for the ultraviolet and germanium for the infrared. Reflective optics can also be tailored for different wavelength intervals and typically consist of glass substrates coated with a metallic layer. Since they do not exhibit chromatic aberration, reflective optics are particularly useful when large wavelength intervals are covered, as in mid-infrared microspectroscopy.

A standard optic in a reflective microscope is the Schwarzchild (also referred to as Cassegrainian) lens; it can be used as both a condenser and an objective. As depicted in **Figure 2b**, the Schwarzchild lens is centrally obscured, which reduces the amount of light collected compared with a refractive optic of similar dimensions. Since the optic is reflective, chromatic aberration is not a concern, but the spherical design can lead to image warping.

It is standard to label objectives with the numerical aperture, *NA*, which is a measure of the light-gathering capability of an optic:

$$NA = n \sin \phi_{\max} \qquad [1]$$

where n is the refractive index of the medium between the sample and objective and $\phi_{\max}$ is the half-angle of the maximum cone of light collected by the lens (see **Figure 3**). In a given apparatus, the *NA* of the objective, relay optics and spectrometer aperture are matched for optimum light collection.

Vibrational objectives typically operate in air, which has a refractive index near unity; the highest *NA* value obtained in air is approximately 0.95 using refractive visible objectives. By changing the surrounding medium, and thus n, it is possible to obtain values greater than 0.95. Immersion objectives operating under media such as water or oil achieve *NA* values greater than 1. For mid-infrared applications, the maximum *NA* for reflective objectives is approximately 0.65. For optimal image formation, it is important to follow the manufacturer's specifications for thickness and refractive index of slides and coverslips (if applicable).

Spatial Resolution

Diffraction effects influence the spatial resolution of a vibrational microspectroscopic measurement. To illustrate consider, for example, monochromatic light from a point source as it propagates through the objective. The image that forms at the focal plane of the objective is not a point, but rather a diffraction pattern consisting of alternating light and dark concentric circles. The bright central disc in the pattern is known as the Airy disc, with a radius r_A given by

$$r_A \approx 0.61\, \lambda / NA_{obj} \qquad [2]$$

where λ is the wavelength of light and *NA* is the numerical aperture of the optic.

Two incoherent point sources of equal brightness lying in a plane perpendicular to the objective are just resolved when

$$R \approx 1.22\, \lambda / (NA_{obj} + NA_{cond}) \qquad [3]$$

where R is the distance between the two points and NA_{obj} and NA_{cond} are the numerical apertures of the objective and condenser, respectively. Equation [3] is known as the Rayleigh criterion, and is a standard measure of the lateral spatial resolution. For an epi-illumination measurement, eqn [3] is recast as

$$R \approx 0.61\, \lambda / NA_{obj} \qquad [4]$$

From eqns [3] and [4], it is seen that the optimum spatial resolution is obtained when objectives with high *NA* are used for measurements at short wavelengths.

The spatial resolution criteria given in eqns [3] and [4] apply for diffraction-limited microscope objectives in the far-field limit. In recent years, near-field techniques have been devised that exceed the diffraction limit by scanning a tapered light source, with a spot size less than the probe wavelength, in close proximity to the sample.

Spectrometers

Dispersive elements and interferometers are widely used in vibrational microspectroscopy. As in bulk measurements, microscopic Raman studies are carried out with grating monochromators, spectrographs or Fourier transform spectrometers. Infrared microspectroscopy, by contrast, is almost exclusively a Fourier transform technique.

At visible and near-infrared wavelengths, vibrational microspectroscopy is also implemented with solid-state filters, particularly in imaging applications. Electronically driven devices such as acousto-optic and liquid crystal filters provide the tunability and moderately narrow passbands required for spectroscopic imaging. These high-speed filters contain no moving parts and can be

custom-built to provide spectral resolutions of less than $10\,cm^{-1}$ over large spectral ranges. Acousto-optic tunable filters (AOTFs) consist of a piezoelectric transducer bonded to a birefringent crystal such as TeO_2. When an RF frequency is applied to the crystal, an acoustic wave is generated that diffracts light over a narrow spectral interval. The AOTF passband is modified by varying the input RF frequency.

Another useful solid-state device is an interference filter fabricated from a set of liquid crystals. The birefringent properties of a liquid crystal tunable filter (LCTF) can be varied by applying an external voltage across a crystal axis. A filter is constructed from a series of polarizers and liquid crystals. A particular passband is selected by tuning the individual liquid crystal elements.

Thin-layer interference filters with passbands between 18 and $50\,cm^{-1}$ are also applied in microspectroscopic imaging. These devices can be tuned over large wavenumber ranges by varying the angle of incidence. Broader wavelength coverage may be obtained with a series of filters, which can be placed in a device such as a filter wheel.

Detectors

The detectors used in vibrational microspectroscopy operate by transducing either the capture of a photon or a minute change in temperature into an electrical response. Both photon and thermal detectors are used individually or configured into an array. The single-point detectors that comprise the array detector are known as picture elements or pixels. **Table 1** lists the wavelength ranges and operating temperatures of several array detectors that are used in Raman and infrared microspectroscopy and imaging.

For the visible to near-infrared region, charge-coupled device (CCD) detectors have been widely adopted for single-point, mapping and imaging Raman microspectroscopy. These photosensitive arrays, in most cases, are monolithic silicon devices that can be fabricated with millions of individual pixels. The wavelength response of CCDs generally declines in the red, cutting off at about 1.1 μm the band-gap of silicon. For this reason, CCDs have limited application in near-infrared microspectroscopy.

For infrared microspectroscopy, single-element detectors are used for point and mapping measurements. More recently, array detectors have been applied for spectroscopic imaging. In infrared focal plane arrays, the monolithic silicon design used in CCDs is replaced by a hybrid construction. In a hybrid detector, photon detection occurs in a semiconductor layer (indium antimonide, mercury cadmium telluride and doped silicon are typical detector materials), while the readout and amplification stages are carried out in a silicon layer. The two layers are electrically connected at each pixel through indium 'bump-bonds'. Other innovations such as microbolometer arrays also show promise for spectroscopic imaging applications.

Raman Microspectroscopy

Point Microscopy

Raman microspectroscopy is routinely implemented using epi-illumination. As shown in **Figures 4**, the objective directs the laser excitation onto the sample and collects the light scattered from the surface. Often fibre optics are used for safe and convenient optical coupling of the microscope to the laser and spectrometer. In point microspectroscopy (**Figure 4**), the Raman signal from a small spot on the sample is dispersed by a grating spectrometer and focused onto a CCD detector. The constituent wavelengths are measured by one or more pixels along a long narrow strip on the CCD. The undesired Rayleigh scattered light, corresponding to the laser excitation wavelength, is removed by placing one or more holographic or dielectric notch rejection filters between the microscope and the spectrometer. Various grating designs, such as dual-stage and subtractive monochromators, also may be used to remove the laser excitation, but are less optically efficient than instruments that incorporate notch rejection filters and single-stage monochromators.

Confocal Raman Microscopy

Optical sectioning of a sample may be achieved with confocal Raman microscopy. This technique rejects out-of-focus light by introducing pinhole apertures into the optical train of the microscope. A confocal scheme is shown in **Figure 5**, where one aperture is placed between the laser and the objective, and another is placed at the image plane of the objective. The apertures block the light scattered from regions outside the focal plane of the objective. Crisp images of thin optical sections may be obtained by mapping the sample point by point. Furthermore, a three-dimensional

Table 1 Properties of various array detectors

	CCD	*InGaAs*	*Pt:Si*	*InSb*	*HgCdTe (MCT)*	*Si:As*	*Microbolometer*
Wavelength range (μm)	300–1.1	0.9–1.7	1–5.7	0.5–5.4	0.8–12.5	1–25	8–14
Operating temperature (K)	77	300	77	77	77	<10	300

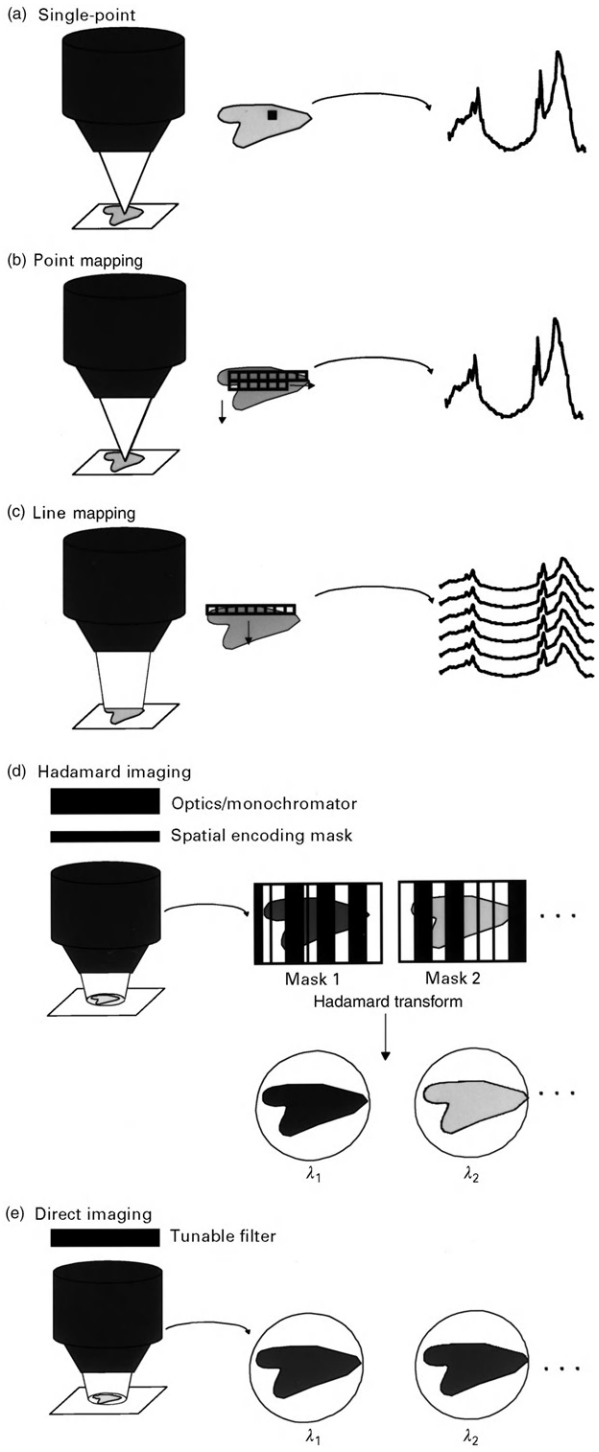

Figure 4 Several different approaches employed in vibrational microspectroscopy. (a) Point measurements: vibrational spectra are obtained at individual, selected points within the sample. (b) Point mapping: spectra are recorded at successive spots within the sample. (c) Mapping is also carried out with line excitation. (d) Spatial encoding methods such as Hadamard transform imaging: a physical mask blocks part of the signal from reaching the detector. A series of images is obtained with the mask in different positions, and then the data are converted to wavelength-dependent images through a Hadamard transform. (e) Direct imaging: the spectroscopic image is obtained by recording the signal from all points on the sample simultaneously over a narrow spectral interval. A series of images at discrete wavelengths is recorded to provide spectroscopic information for each pixel.

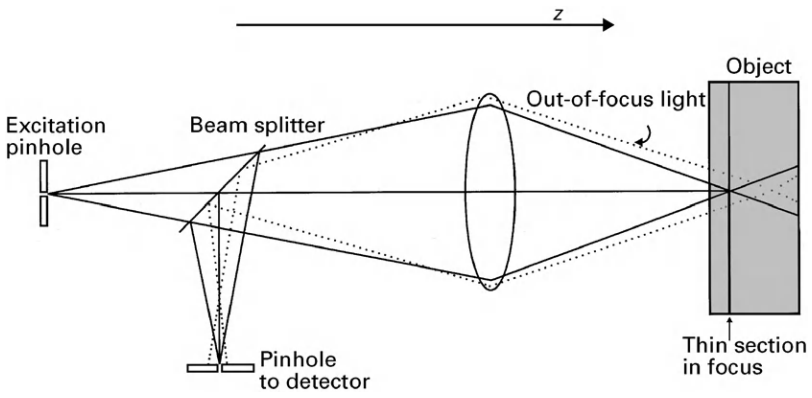

Figure 5 Confocal microscopy: pinhole apertures placed in the optical train of the microspectrometer lead to rejection of out-of-focus light.

image of the sample may be constructed by carrying out measurements at different sample depths.

Mapping

Mapping techniques scan the excitation source or the sample in a raster or line pattern (see **Figures 4b** and **4c**). In a raster scan, spectra may be recorded at successive points by moving either the sample or source on a motorized platform. Mapping may also be implemented by irradiating the specimen with a line source. In one method, a line is produced by rapidly sweeping the laser beam back and forth with a mirror powered by a piezoelectric transducer. It is also possible to focus the laser beam into a line with cylindrical optics. High-precision designs for mapping apparatus minimize mechanical instabilities and positioning errors.

For point mapping, the Raman signal is recorded as in single-point measurements. When the excitation is along a line, the Raman signal is collected through the objective, directed onto a grating and dispersed on to a CCD. The two-dimensional detector then records the spatial information along one axis and wavelength data along the other. An image cube is gradually built up as the line is moved across the full sample area.

Imaging

As shown in **Figures 4d** and **4e**, point and line excitation are replaced by wide-field irradiation in both spatial encoding and direct imaging methods. In a common arrangement, a given sample area is illuminated by defocusing the laser through a beam expander prior to the objective. The sample illumination is not perfectly uniform in this configuration because the intensity distribution of the laser beam (typically Gaussian) is preserved. Other properties of monochromatic coherent excitation may also affect the image quality. Despite the experimental concerns, wide-field illumination is useful when dealing with fragile specimens, since the power density is reduced, thus minimizing damage from thermal or photolytic processes.

Hadamard Transform Imaging

Spatial encoding methods such as Hadamard transform imaging also can be used for the spectroscopic visualization of samples. More recently, developments in digital microarray technology will likely provide a convenient new approach for spatial encoding from the mid-infrared to the ultraviolet. In one common arrangement, the entire sample area is irradiated with wide-field, epi-illumination (**Figure 4d**). Part of the Raman signal emanating from the sample is blocked with a mask containing a series of apertures. The spatially filtered signal is focused on to an entrance slit of a monochromator, which disperses the signal across a two-dimensional array detector. The slit preserves one image axis while the Hadamard mask is used to encode the other axis. Subsequent measurements are carried out with the mask in different positions. Each measurement corresponds to the Raman signal from the unmasked points on the sample along one spatial axis over the entire spectral range of interest. The experiment is designed such that the number of independent measurements equals the number of points on the sample. The spatially dependent images are then converted to spectroscopic images through a Hadamard transform. Unlike the other methods mentioned in this article, Hadamard spectroscopic imaging systems are limited to research activities and are not yet commercially available.

Direct Imaging

Raman microscopic imaging can also be carried out by imaging the sample through an interferometer or filter (shown in **Figure 4e**). The sample is irradiated with wide-field, epi-illumination and then modulated or filtered images are recorded with a CCD. Spectroscopic information is obtained by recording sequential images over a range of optical retardations in the case of the

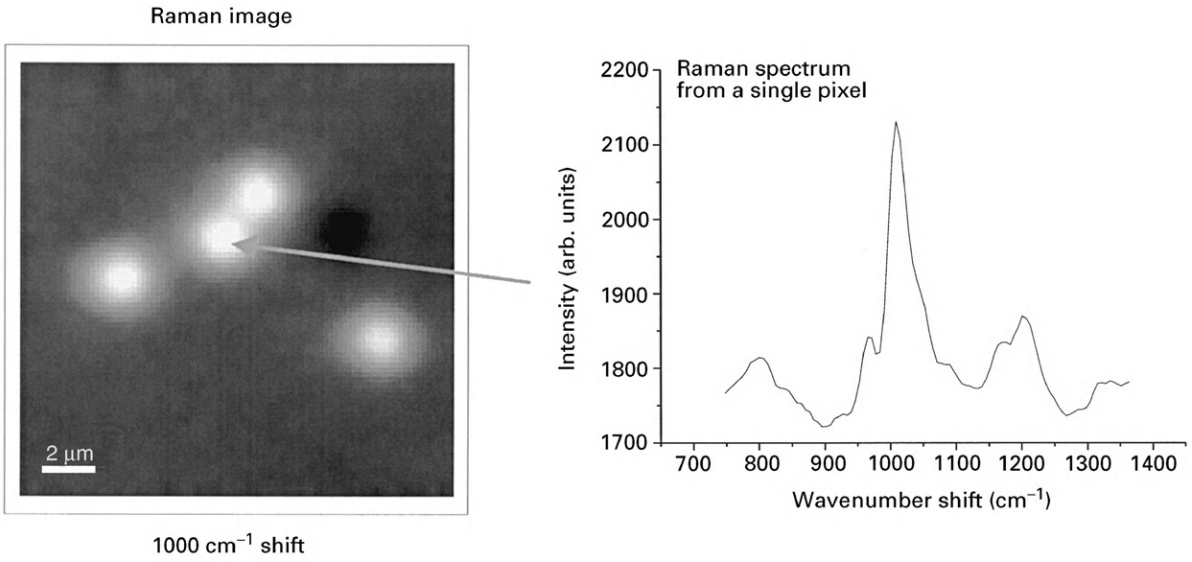

Figure 6 A Raman spectroscopic image of 1 μm diameter polystyrene beads. The spectroscopic image on the left exhibits bright regions that correspond to the Raman signal at 1000 cm^{-1} shift, a symmetric aromatic ring vibration. A series of images was recorded between 747 and 1363 cm^{-1} shift; a spectrum is then available for every spatial resolution element in the image. The trace on the right corresponds to the spectrum of a single pixel from the centre of a single polystyrene bead.

interferometer or a range of frequencies in the case of the tunable filter. In this way, spectra corresponding to various points within the sample are obtained at each detector pixel. Since the image is captured in its entirety, the results are not prone to mechanical positioning errors that may occur in point or line mapping methods. The image quality, in fact, is primarily limited by diffraction. When image shifts occur in direct imaging, they are usually predictable and can be compensated by either experimental or computer procedures.

The basic principles of Raman microscopy and imaging are encapsulated by Figure 6, which depicts a Raman image and a spectrum of a 1 μm diameter polystyrene bead. The data were obtained with a microscope coupled to a CCD array; individual images were recorded through an AOTF, which was successively tuned between 747 and 1363 cm^{-1} from the exciting 647 nm Kr^+ laser line. The Raman image shown was recorded at 1000 cm^{-1}, corresponding to a symmetric aromatic ring vibration in polystyrene. The bright areas correspond to areas rich in polystyrene, thus revealing the distribution of beads in the sample. A spectrum for every pixel is available because images were recorded over a series of wavelengths. Figure 6 illustrates a spectrum obtained from a single pixel in one of the bead centres.

Infrared Microspectroscopy

Infrared microspectroscopy is based on either transmission or reflection measurements. Transmission is the simplest implementation; the maximum sample thickness is sample and wavelength dependent, however, and is limited to approximately 15–20 μm for mid-infrared measurements. Reflection measurements are indispensable for samples that are thick or opaque. Various microscope objectives have been tailored for measurements based on the corresponding bulk infrared techniques, such as diffuse reflectance attenuated total reflectance and grazing angle reflectance.

Optical effects such as stray light or scattering are treated by placing one or more apertures in the optical train of the infrared microscope. For transmission measurements, one aperture is placed between the condenser and the sample and another is placed between the objective and the image plane. The two apertures are matched in size in order to optimize the signal. For reflectance measurements, only one aperture is used. This type of arrangement is widely employed in infrared spectroscopy, and is known as 'redundant aperturing'.

Single-Point Measurements

Most single-point infrared microspectroscopy is implemented with Fourier transform spectrometers, for which the well-known multiplex and throughput advantages generally apply. The multiplex advantage arises because all of the input radiation is detected over the entire scan time; however, it applies only when the dominant source of noise is the detector. When the detection is shot-noise limited, as with CCDs, the multiplex advantage does not hold. The throughput advantage for interferometers arises from the use of circular apertures. Dispersive instruments, by contrast, require narrow exit and

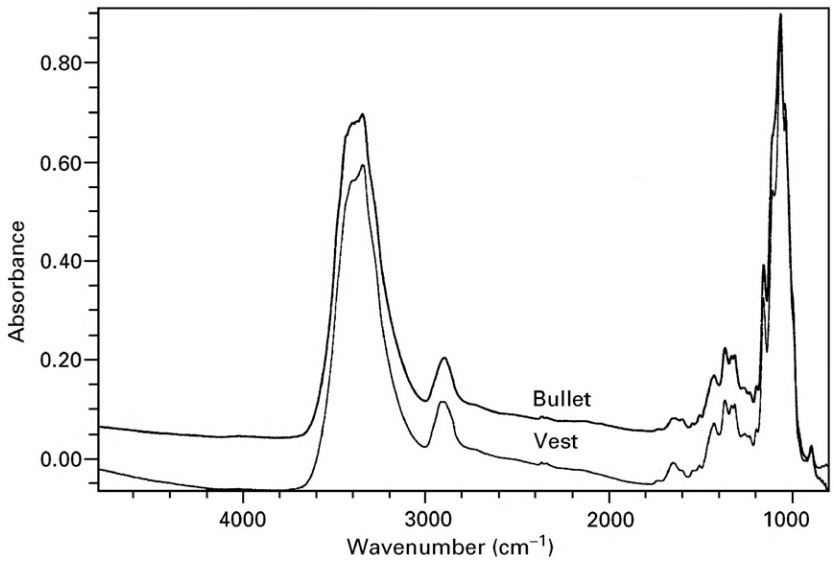

Figure 7 Infrared microspectra of cotton fibres collected in a forensic application. The spectrum of a fibre retrieved from a bullet (top trace) is seen to match the spectrum of a fibre from the police officer's vest (bottom trace). Data courtesy of John A. Reffner, Spectra-Tech, Inc. and Ronald P. Kaufman, Maine State Police Crime Laboratory.

entrance slits, particularly for higher spectral resolution. Furthermore, a circular aperture provides a more convenient geometry for coupling a microscope to the spectrometer.

Trace amounts of sample can be analysed with infrared microspectroscopy. The technique, for example, is a standard tool in forensic science. **Figure 7** illustrates fibre spectra that were key evidence in a criminal investigation. A cotton fibre fragment, which was recovered from the nose of a bullet, was matched spectroscopically to fibres from the vest of a police officer who had been shot. Fibre samples represent a system that is difficult to examine with bulk techniques, but which is amenable to vibrational microscopic analysis.

Mapping and Imaging

Infrared mapping and imaging approaches are applied as in the corresponding Raman approaches, with the appropriate choices for source, spectrometer, and detector. For example, a combination of an acousto-optic filter and an InSb focal plane array can be used to record frequency-dependent images in the near-infrared. In the mid-infrared, direct images are recorded with a step-scan interferometer coupled to an infrared focal plane array detector. To illustrate, consider a transmission measurement in which a step-scan interferometer modulates the output from a blackbody source. The infrared radiation is directed on to the sample with the condenser. The transmitted infrared radiation is collected by the objective and then focused on to the array detector. Over the course of the scan, the movable mirror in the interferometer is paused for several milliseconds at every step in order to record the image. At the completion of a single scan, a complete interferogram is generated at each detector pixel. The interferograms are then converted to frequency by standard Fourier transform processing.

As an example of the Fourier transform infrared imaging technique, **Figure 8** depicts an infrared spectroscopic image of human breast cells which was recorded with a 64×64 mercury–cadmium–telluride (MCT) array. The data set then encompasses 4096 separate interferograms, one for each pixel. Spectra are obtained through standard Fourier transform procedures. The resulting data cube contains the set of image planes stacked as a function of frequency. Each image exhibits contrast based on the differences in infrared spectral response, which in turn reflects the variation in the chemical composition within the sample. **Figure 8** depicts one such image plane at 2927 cm^{-1}, which corresponds to a protein and lipid infrared molecular marker (CH_2 antisymmetric stretch). In this way, the distribution of biochemical species can be visualized across the sample. More detailed chemical information can be obtained by examining the infrared spectra that are associated with each pixel in the image.

Sampling Considerations in Image Generation

The Nyquist theorem specifies that a sinuisoidal function in time or distance can be regenerated with no loss of information as long as it is sampled at a frequency greater than or equal to twice per cycle. The Nyquist theorem

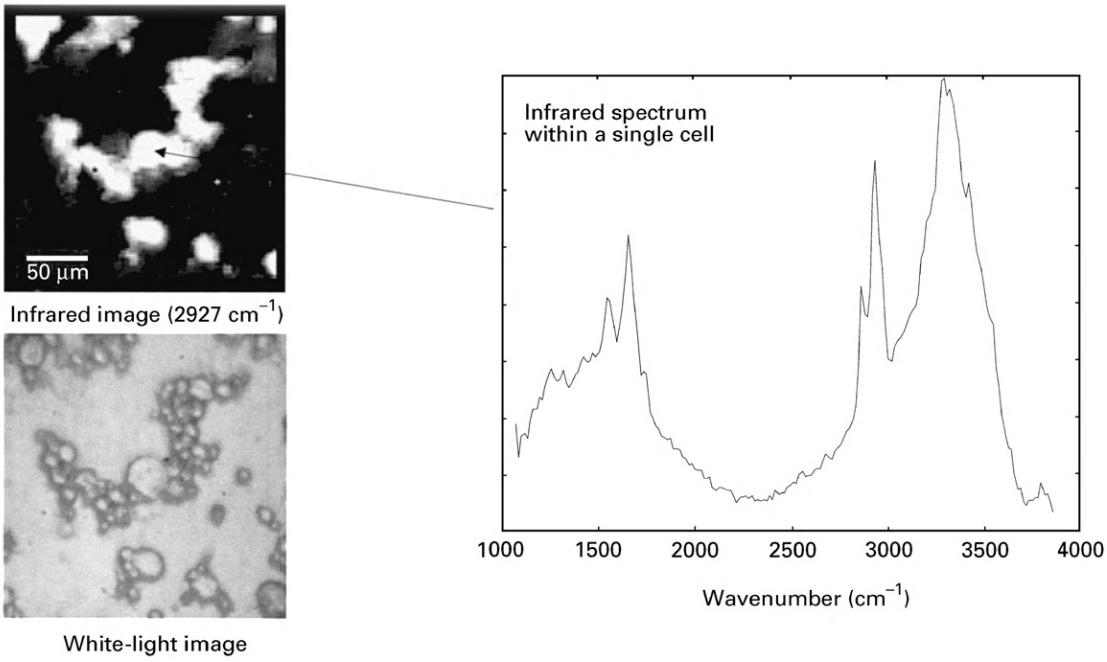

Figure 8 An infrared spectroscopic image of human breast cells. The spectroscopic image on the left exhibits contrast based on the intensity of the absorption band centred at 2927 cm^{-1} (antisymmetric CH_2 stretch), which contains contributions from both the lipid and protein fractions within the cell. Since images are obtained over a contiguous wave number interval, it is possible to construct a spectrum for every image pixel. The spectrum extracted from one of the cells is shown on the right.

must be considered in direct imaging applications because the signal is sampled by the discrete pixel elements in an array. Consider a diffraction-limited arrangement with a lateral spatial resolution R_L. If the total magnification M_{tot} is a product of the magnifications of the microscope objective M_{obj} and the projection lens M_{proj}, the Nyquist theorem requires

$$M_{tot}R_L \geq 2p \qquad [5]$$

where p is the pixel size. That is, the sampling interval must be at least twice the highest spatial interval. If the smallest resolvable feature is 5 μm, then each detector pixel must sample intervals that are ≤ 2.5 μm. As long as eqn [5] is obeyed, the spatial fidelity of the microscopic image is preserved and sampling artifacts are avoided. It follows that oversampling does not provide any additional information; this is also known as empty magnification.

See also: IR Spectrometers, Light Sources and Optics, Raman Spectrometers, Scanning Probe Microscopes, Surface Studies by IR Spectroscopy.

Further Reading

Humecki HJ (ed.) (1995) *Practical Guide to Infrared Microspectroscopy*. New York: Marcel Dekker.

Inoué S and Oldenburg R (1995) Microscopes. In: van Stryland EW, Williams DR, and Wolfe WL (eds.) *Handbook of Optics*, vol. II, pp. 17.1–17.52. New York: McGraw-Hill.

James J and Tanke HJ (1991) *Biomedical Light Microscopy*. Dordrecht: Kluwer Academic Publishers.

Katon JE (1996) Infrared microspectroscopy: A review of fundamentals and applications. *Micron* 27: 303–314.

Katon JE and Summer AJ (1992) IR microspectroscopy. *Analytical Chemistry* 64: 931A–940A.

Laserna JJ (ed.) (1996) *Modern Techniques in Raman Spectroscopy*. Chichester: Wiley.

Lewis EN, Treado PJ, Reeder RC, et al. (1995) Fourier transform spectroscopic imaging using an infrared focal-plane array detector. *Analytical Chemistry* 67: 3377–3381.

Messerschmidt RG and Harthcock MA (eds.) (1998) *Infrared Microspectroscopy: Theory and Applications*. New York: Marcel Dekker.

Puppels GJ, de Mul FFM, Otto C, et al. (1990) Studying single living cells and chromosomes by confocal Raman spectroscopy. *Nature* 347: 301–303.

Reffner JA (1998) Instrumental factors in infrared microspectroscopy. *Cellular and Molecular Biology* 44: 1–7.

Rieke GH (1994) *Detection of Light: From the Ultraviolet to the Submillimeter*. Cambridge: Cambridge University Press.

Turrell G and Corset J (eds.) (1996) *Raman Microscopy: Developments and Applications*. London: Academic Press.